DESIGN AND ANALYSIS OF A NOVEL ELECTROMAGNETIC BANDGAP STRUCTURE FOR SUPPRESSING SIMULTANEOUS SWITCHING NOISE

H. M. Lu[1, *], J. X. Zhao[1], and Z. Y. Yu[2]

[1]School of Electronic Engineering, Xidian University, Xi'an 710071, China

[2]Institute of Scientific Research Ministry, Engineering University of The Second Artillery, Xi'an 710025, China

Abstract—An electromagnetic bandgap (EBG) structure is proposed to suppress the simultaneous switching noise (SSN) from 0.45 GHz to 5.3 GHz with an averaged suppression level of -66.4 dB. The design is based on the inductance enhancement by using meander lines to bridge slotted metal patches embedded into the power plane. Numerical simulation and experimental measurement are both used in the study for mutual verification. Compared to the conventional L-bridged EBG structure, the novel design increases the bandwidth by 15% and reduces the lower frequency by 150 MHz. A better omnidirectional SSN suppression is also achieved. For high-speed digital applications, the signal integrity is analyzed and improved.

1. INTRODUCTION

Simultaneous switching noise (SSN) is a bottleneck in the application of modern high-speed digital circuits with fast edge rates and clock frequencies [1]. SSN reduces the noise margin and undermines the performance of analog circuits in the system with mixed signals. The noise from the simultaneous switching of multiple devices induces the voltage fluctuation of the power distribution system, which conversely reduces the signal integrity and causes problems of electromagnetic compatibility [2].

In the last decade, various measures are taken to relieve the SSN, including adding lumped capacitors between the power and ground

planes, selecting the location of via ports, and employing differential interconnecting circuits, etc [3].

Decoupling capacitors restrict the SSN-induced voltage fluctuation by reducing the high-frequency impedance of the power or ground plane. However, this technique has a frequency limit. Beyond 600 MHz, the application is basically not effective due to the series resonance of the capacitance and the equivalent inductance [4]. Typical SSN has a low-pass spectrum up to 6 GHz, most of which is not covered by the bypassing frequencies of decoupling capacitors.

In recent years, SSN with the spectrum beyond the decoupling range of capacitors is reduced by a novel technique using the high impedance surface. The design is based on the electromagnetic bandgap (EBG) and photonic bandgap (PBG) structures. EBG structures with mushroom-shaped cells and coplanar cells are proposed to inhibit the propagation of cavity-resonance modes and noises [5, 6]. The mushroom-shaped EBG structure uses a layer of periodical metal patches between the power and ground planes. The patches are connected to the ground plane by specially designed connecting vias. Inserted dielectric substrate helps to reduce the size of the structure. The coplanar EBG structure is composed of metal patches embedded in the power plane with bridges between adjacent patches. Compared to the mushroom-shaped EBG structure, the coplanar EBG structure are cost-effective by using standard design and production techniques of printed circuit board (PCB). The power plane with L-bridged coplanar EBG structure provides a 4 GHz bandwidth for SSN suppression from 0.60 GHz to 4.6 GHz [7]. Hybrid EBG structures with lumped chip capacitors and inductors are later developed to reduce the cutoff frequency and expand the suppression bandwidth [8]. Ultra-wideband SSN suppression between 1 GHz and 40 GHz is realized by the combination of low- and high-frequency EBG cells [9]. The coating of a magnetic material over the EBG structure is proved to shift the bandgap toward lower frequencies and improve the SSN propagation loss [10]. The addition of an adjustable air-gap beneath the substrate of the PCB helps to achieve tunable performances of the SSN suppression [11]. In high-speed digital circuits, the meander-line bridging is a novel design of the coplanar EBG structure. Developed from the L-bridged EBG structure, various meander-line EBG structures have promised a feasible and effective technique for SSN suppression [12–14].

In this paper, an MS-EBG structure is introduced into the power plane of the PCB. The structure is featured by the addition of Z-shaped slots etched into square metal patches bridged by meander lines. Numerical simulations and experimental measurement are

used to examine the performance of the novel design. Compared to conventional L-bridged EBG structures, the combination of slots and meander-line bridges of the MS-EBG structure achieves a bandwidth increase of 15% for an improved SSN suppression level of $-66.4\,\mathrm{dB}$ [7, 12, 13]. The novel design also proves an omnidirectional SSN suppression and minimum influence on the signal integrity.

2. MODEL AND METHODS

2.1. MS-EBG Structure

In high-speed digital circuits, the power and ground planes are embedded into the PCB with multiple circuit layers. To maintain the signal integrity, the power and ground planes are required to be continuous layouts for the direct current. High superficial resistivity on these planes is expected to efficiently filter out the alternating noise [1, 4]. Dimensionally much smaller than the wavelength, the cell of the EBG structure functions as a band-stop filter and is recognized as a parallel resonant circuit quantified by the capacitance C and inductance L. Both parameters are determined by the geometry of the metal patch and the bridge: the gap between neighboring patches provides C, whereas L is introduced by the bridge. The central frequency of the suppression band is quasi-quantitatively described by $(2\pi\sqrt{LC})^{-1}$. The relative bandwidth is in direct proportion to
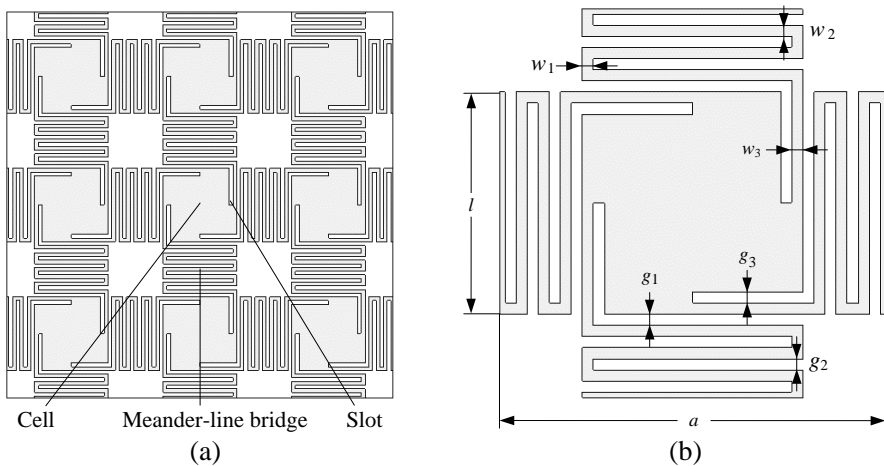
Figure 1. (a) MS-EBG structure with meander-line bridges and slots. (b) Geometry parameters of a cell.

$\sqrt{L/C}$. Based on these principles, an EBG structure with better SSN suppression is possible if we geometrically increase the inductance and decrease the capacitance to reduce the central frequency and expand the relative bandwidth.

The EBG structure of this study is characterized by the inductance enhancement with bridges of meander lines and slots etched into the metal patch. The configuration is named meander-line-slot EBG (MS-EBG) structure, shown in Figure 1(a). The EBG structure consists of an array of 3×3 cells. The geometry of a cell is parameterized, as shown in Figure 1(b), where the length of the cell $a = 30\,\text{mm}$; the widths and length of meaner lines are $w_1 = w_2 = w_3 = 0.2\,\text{mm}$ and $l = 27\,\text{mm}$; the gaps are $g_1 = g_2 = g_3 = 0.2\,\text{mm}$.

2.2. Numerical Simulation

A finite element software (Ansoft HFSS) is used in the numerical study of the transmission properties to describe the insertion loss and quantify the SSN suppression of the MS-EBG structure. The MS-EBG structure is embedded into the power plane of a double-layer PCB. The ground plane is a plain sheet. Identical simulation parameters are selected for comparison to previous results from other typical designs. The FR4 substrate has a relative permittivity of 4.4 and loss tangent of 0.02 over the frequency range of interest. The metal layers are silver-gilded copper and parameterized as the perfect electric conductor.

The HFSS model of the PCB with the MS-EBG power plane is shown in Figure 2(a). The size of the PCB is $90\,\text{mm} \times 90\,\text{mm} \times 0.4\,\text{mm}$. Three ports are added into the model. The input is port 1 at

(a)   (b)
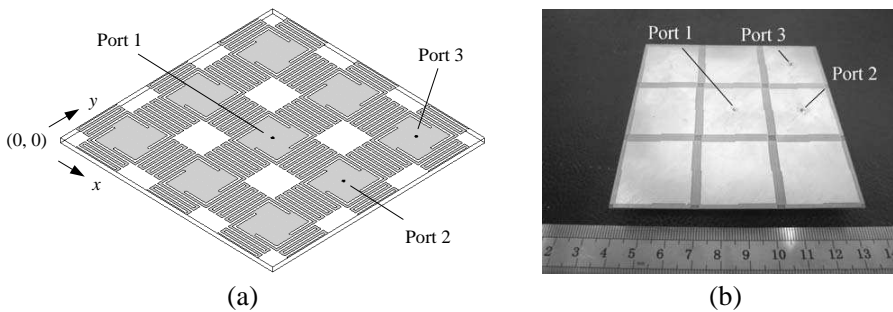
Figure 2. (a) Model of the PCB with the MS-EBG power plane for numerical simulation. (b) Photograph of the PCB with the MS-EBG power plane for experimental measurement.

$(x, y) = (45\,\text{mm}, 45\,\text{mm})$. Two outputs are port 2 at $(75\,\text{mm}, 45\,\text{mm})$ and port 3 at $(75\,\text{mm}, 75\,\text{mm})$. A lumped source is added to the input port and simulates the excitation from a standard $50\,\Omega$ cable. The transmission properties from the input port to the output ports are calculated.

2.3. Experimental Measurement

To validate the accuracy of the HFSS simulation, we use a vector network analyzer (Agilent N5230a) to measure the transmission properties of the MS-EBG power plane. Due to the available material, the thickness of the PCB is $0.5\,\text{mm}$ instead of the previous $0.4\,\text{mm}$. Other geometry dimensions are unchanged. An HFSS simulation of the $0.5\,\text{mm}$ PCB is performed to provide numerical data for comparison.

The photograph of the fabricated PCB with the MS-EBG power plane is shown in Figure 2(b). SMA connectors with $50\,\Omega$ power matching are added to the input port and output ports. The transmission loss of the connectors and cables are measured for compensation.

3. VALIDATION

The comparison between the experimental measurement and the numerical simulation is shown in Figure 3. For the MS-EBG power plane on the $0.5\,\text{mm}$ PCB, a good agreement is found for transmission properties quantified by S_{21} and S_{31} across the frequency range from $0.45\,\text{GHz}$ to $5.3\,\text{GHz}$. The bandwidth parameters are also very close between the experimental and numerical data, as listed in Table 1,
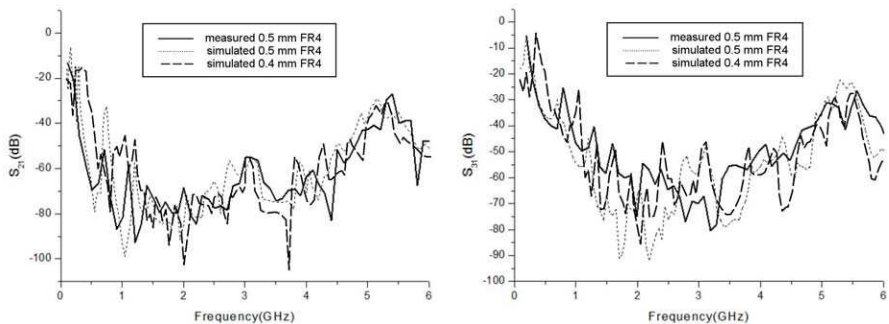
Figure 3. Comparison of S_{21} and S_{31} between the measured and simulated MS-EBG power planes.

**Table 1.** Comparison of the bandwidth parameters between the measured and simulated MS-EBG power planes.

Results	S_{21}		S_{31}	
	$-30\,$dB bandgap (GHz)	Relative suppression bandwidth (%)	$-30\,$dB bandgap (GHz)	Relative suppression bandwidth (%)
Measured	4.96	182	4.78	150
Simulated	4.78	176	4.85	175

where the suppression bandwidth is measured by $-30\,$dB bandgap. Simulated S_{21} and S_{31} results from the MS-EBG power plane on the 0.4 mm PCB are also displayed in Figure 3. It is indicated that the change of the PCB thickness between 0.4 mm and 0.5 mm induces little variance in the transmission properties with no significant influence on the SSN suppression. The validation guarantees the accuracy of the following numerical results of the MS-EBG power plane on the 0.4 mm PCB.

4. RESULTS

4.1. SSN Suppression

For a comparative study on the performance of the MS-EBG power plane, we also consider a reference power plane and an L-bridged EBG power plane. The reference power plane is a plain layout with the same PCB dimensions, as well as the input and output ports. The L-bridged EBG power plane is selected from that in [7] for structural similarity. The suppression bandwidth is still quantified by $-30\,$dB bandgap. Because of the geometry difference, we did not use the meander-line EBG structure proposed in [12], where three cells exist between the input and output ports and the bandwidth is measured by $-28\,$dB. The transmission properties are compared in Figure 4. The SSN suppressions of the MS-EBG and L-bridged EBG power planes are obviously effective. Measured by S_{21}, the 0.60 GHz–4.6 GHz bandgap of the L-bridged EBG power plane is extended to 0.45 GHz–5.3 GHz by the MS-EBG power plane. The lower frequency is reduced by 150 MHz. Similar result of the bandgap expansion is found for S_{31}. The reduction of the lower frequency is expected and in accordance with the theoretical analysis [15]. The lower frequency is inversely proportional to the inductance introduced by the connection between adjacent cells. The addition of the slot etched into the cell helps to increase the
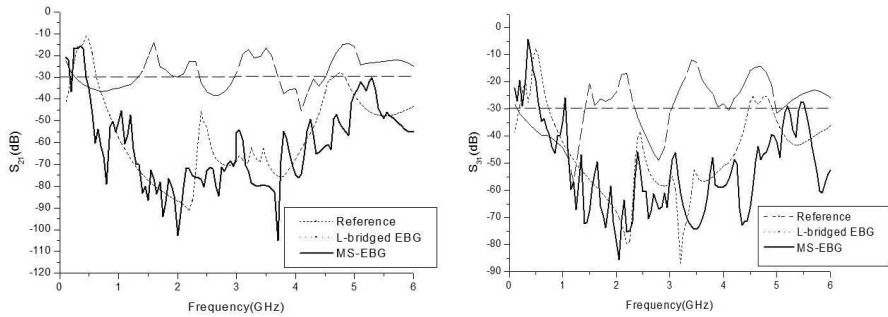
**Figure 4.** Comparison of S_{21} and S_{31} among the reference, L-bridged EBG, and MS-EBG power planes.

Table 2. Comparison of the SSN suppression between the L-bridged EBG and MS-EBG power planes.

Power plane	S_{21}		S_{31}	
	$-30\,\text{dB}$ bandgap (GHz)	Averaged suppression level (dB)	$-30\,\text{dB}$ bandgap (GHz)	Averaged suppression level (dB)
L-bridged EBG	4.00	-62.2	3.65	-52.9
MS-EBG	4.85	-66.4	4.65	-59.3

overall length of the connection and the inductance, thus shifting the lower frequency downward. A quantified comparison between the two EBG power planes is listed in Table 2. Compared to the L-bridged EBG power plane, the MS-EBG power plane expands the relative suppression bandwidth from 154% to 169% (15% absolute expansion) as measured by S_{21}. For S_{31}, the relative suppression bandwidth is expanded from 135% to 163% (28% absolute expansion). For the MS-EBG power plane, the averaged suppression levels are lower than those of the L-bridged EBG power plane. The suppression bandwidths and averaged suppression levels are similar between S_{21} and S_{31}, indicating a better omnidirectional SSN suppression of the novel design.

4.2. Signal Integrity

The wideband SSN suppression of the MS-EBG structure has cost the continuity of the power plane, thus potentially degrading the integrity of the signal in high-speed digital circuits. To evaluate the effect of the structure on the signal integrity, we designed a four-layer PCB, as
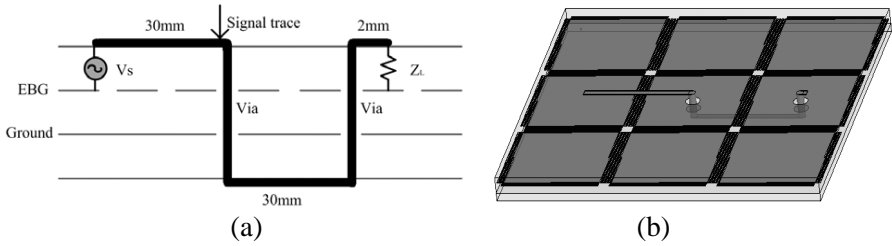
Figure 5. (a) Side view of the four-layer PCB with the signal trace. (b) Configuration of the transmission line.

shown in Figures 5(a) and 5(b). The two inner layers are the power and ground planes, whereas the top and bottom layers are signal planes. A 1-mm-wide transmission line with $50\,\Omega$ characteristic impedance guides the signal from the top plane to the bottom plane and returns to the top through two vias. The signal trace is $64\,\text{mm}$. Ansoft Designer is applied in the analysis. The pseudo-random binary sequence is launched at the source V_s. The sequence is coded at $2.5\,\text{GHz}$. Logic 0 and logic 1 are set at levels of $0\,\text{mV}$ and $500\,\text{mV}$, respectively, with $120\,\text{ps}$ normal rise/fall time. At the $50\,\Omega$ load Z_L, the signal integrity is observed as the eye diagram characterized and quantified by the maximum eye open (MEO) and the maximum eye width (MEW).

Figures 6(a) and 6(b) compare the eye patterns between the reference power plane and the MS-EBG power plane. It is read that the MEO and MEW are $415\,\text{mV}$ and $380\,\text{ps}$ for the reference power plane. For the MS-EBG power plane, the MEO and MEW are reduced to $252\,\text{mV}$ and $361\,\text{ps}$, respectively. The signal integrity is sensitively degraded by the MS-EBG structure. The use of differential pair of transmission lines effectively improves the signal integrity with the MS-EBG application. In Figure 6(c), the single transmission line is replaced by a differential pair of transmission lines. In the geometry, each line is $0.5\,\text{mm}$ wide with the characteristic impedance of $100\,\Omega$. The lines are separated by $0.25\,\text{mm}$. The result of the eye pattern is shown in Figure 6(d). The openness of the eye pattern is improved significantly. The MEO and MEW are $390\,\text{mV}$ and $373\,\text{ps}$. Compared to the reference power plane, the reductions of MEO and MEW are 6.0% and 1.8%, respectively, indicating a minimum influence on the signal integrity of the MS-EBG power plane with the use of differential pair of transmission lines.
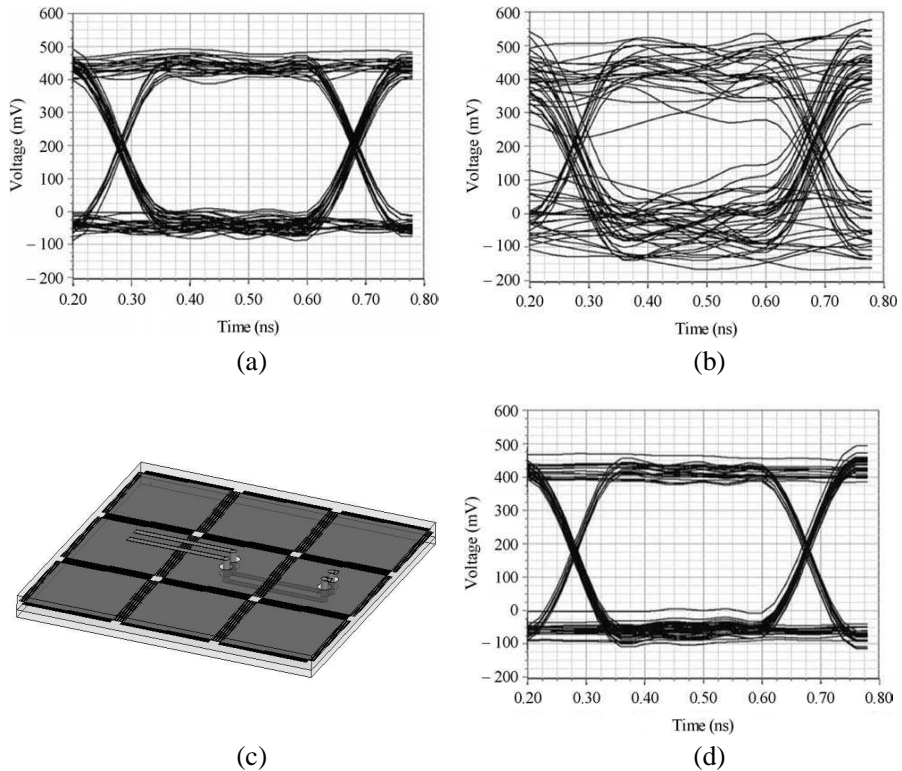
Figure 6. (a) Eye diagram of the reference power plane. (b) Eye diagram of the MS-EBG power plane. (c) Configuration of the differential pair of transmission lines. (d) Eye diagram with the use of differential pair of transmission lines on the MS-EBG power plane.

5. CONCLUSION

The proposed MS-EBG structure enhances the inductance for wideband SSN suppression by using the combination of meander-line bridge connections and slots etched in metal patches. Supported by experimental measurement, the numerical simulation of the power plane with the novel design shows an effective SSN suppression from 0.45 GHz to 5.3 GHz. The suppression bandwidth is expanded by 15% and the lower frequency is reduced by 150 MHz, as compared to the L-bridged EBG power plane of the same geometry. The MS-EBG power plane has a far better omnidirectional SSN suppression. The signal integrity is improved to minimum MEO and MEW variances with the use of differential pair of transmission lines.

ACKNOWLEDGMENT

REFERENCES

1. Swaminathan, M., J. Kim, I. Novak, and J. P. Libous, "Power distribution networks for system-on-package: Status and challenges," *IEEE Transactions on Advanced Packaging*, Vol. 27, No. 2, 286–300, May 2004.

2. Van den Berghe, S., F. Olyslager, D. De Zutter, J. De Moerloose, and W. Temmerman, "Study of the ground bounce caused by power plane resonances," *IEEE Transactions on Electromagnetic Compatibility*, Vol. 40, No. 2, 111–119, May 1998.

3. Abhari, R. and G. V. Eleftheriades, "Metallo-dielectric electromagnetic bandgap structures for suppression and isolation of the parallel-plate noise in high-speed circuits," *IEEE Transactions on Microwave Theory and Techniques*, Vol. 51, No. 6, 1629–1639, June 2003.

4. Wu, T. L. and T. K. Wang, "Embedded power plane with ultra-wide stop-band for simultaneously switching noise on high-speed circuits," *Electronics Letters*, Vol. 42, No. 4, 213–214, February 2006.

5. Sievenpiper, D., L. Zhang, R. F. J. Broas, N. G. Alexópolous, and E. Yablonovitch, "High-impedance electromagnetic surfaces with a forbidden frequency band," *IEEE Transactions on Microwave Theory and Techniques*, Vol. 47, No. 11, 2059–2074, November 1999.

6. Lu, H. M., X. L. Zhang, Z. Y. Yu, and Y. M. Zhao, "Wideband GBN suppression in high-speed printed circuit boards and packages using double-side electromagnetic band-gap structure," *The 8th International Symposium on Antennas, Propagation and EM Theory*, 1093–1095, Kunming, China, 2008.

7. Wu, T. L., C. C. Wang, Y. H. Lin, T. K. Wang, and G. Chang, "A novel power plane with super-wideband elimination of ground bounce noise on high speed circuits," *IEEE Microwave and Wireless Components Letters*, Vol. 15, No. 3, 174–176, March 2005.

8. Kim, K. H. and J. E. Schutt-Ainé, "Analysis and modeling of hybrid planar-type electromagnetic-bandgap structures and

feasibility study on power distribution network applications," *IEEE Transactions on Microwave Theory and Techniques*, Vol. 56, No. 1, 178–186, January 2008.

9. Rao, P. H., "Hybrid electromagnetic bandgap power plane for ultra-wideband noise suppression," *Electronics Letters*, Vol. 45, No. 19, 981–982, September 2009.

10. Eom, D.-S., J. Byun, and H.-Y. Lee, "New structure of composite power plane using spiral EBG and external magnetic material for SSN suppression," *Progress In Electromagnetics Research Letters*, Vol. 15, 69–77, 2010.

11. Veysi, M. and M. Shafaee, "EBG frequency response tuning using an adjustable air-gap," *Progress In Electromagnetics Research Letters*, Vol. 19, 31–39, November 2010.

12. Qin, J., O. M. Ramahi, and V. Granatstein, "Novel planar electromagnetic bandgap structures for mitigation of switching noise and EMI reduction in high-speed circuits," *IEEE Transactions on Electromagnetic Compatibility*, Vol. 49, No. 3, 661–669, August 2007.

13. Oh, S. S., J. M. Kim, J. H. Kwon, and J. G. Yook, "Enhanced power plane with photonic band gap structures for wide band suppression of parallel plate resonances," *2005 IEEE Antennas and Propagation Society International Symposium*, Vol. 2B, 655–658, 2005.

14. He, H.-S., X.-Q. Lai, Q. Ye, Q. Wang, W.-D. Xu, J.-G. Jiang, and M.-X. Zang, "Wideband SSN suppression in high-speed PCB using novel planar EBG," *Progress In Electromagnetics Research Letters*, Vol. 18, 29–39, September 2010.

15. Kim, K. H. and J. E. Schutt-Ainé, "Design of EBG power distribution networks with VHF-band cutoff frequency and small unit cell size for mixed-signal systems," *IEEE Microwave and Wireless Components Letters*, Vol. 17, No. 7, 489–491, July 2007.